

A THERMORESPONSIVE ELECTROMECHANICAL MICROCHIP FOR TEMPERATURE CONTROL IN BIOMEDICAL SMART IMPLANTS

Anindya L. Roy and Kenichi Takahata

Department of Electrical and Computer Engineering
University of British Columbia, Vancouver, B.C., CANADA

ABSTRACT

This paper reports an electromechanical micro circuit breaker device developed for self-temperature regulation and safe operation of electronic implants that produce heat *in vivo*. A micromachined cantilever actuator made of nitinol is used as a normally closed thermoresponsive switch to prevent the host implant from overheating. The device is packaged to be a biocompatible microchip with a footprint of $0.7 \times 1.9 \text{ mm}^2$. The testing of fabricated microchips shows their contact resistance of $\sim 35 \Omega$ at the cold state and rapid rise to the open state as temperature reaches $\sim 54^\circ\text{C}$. Their electromechanical responses to heat and related threshold temperatures are measured to be well consistent with those of the particular nitinol material used. These preliminary results illustrate the desired functionality of the micro circuit breaker, validating the effectiveness of the adopted design-fabrication approach.

INTRODUCTION

The electronic “smart” medical implants and wearable microdevices, enabled by micro-electro-mechanical systems (MEMS) technology with an aid of integrated microelectronics, have been reported with great potential for a variety of applications, including implantable drug delivery devices, telemetric stents and an extensive range of implantable and wearable sensors [1-3]. Thermal management is a critical requirement in these medical devices. The embedded circuitry, powered either internally (e.g., with batteries) or externally (e.g., by electromagnetic power transfer) generates heat during its operation based on Joule’s first law, elevating device temperature while causing irreversible power loss. This type of thermal issue deteriorates with the integration of more functions in a device, leading to the need for greater powers and heat dissipation. Thermal trauma is a critical risk associated with these devices that could cause permanent cellular damage due to excessive heat transfer to surrounding tissue [4]. Thus, temperature regulation in smart implants that dissipate heat will be an essential task for the sake of safety. This need exists especially in implantable MEMS that are driven by electrothermal mechanisms [5]. Although thermal management could be implemented using temperature sensors with active electronics, this is generally difficult to achieve in implants where the available space is highly limited. The use of passive components that offer a self-temperature regulation function will be a promising path to address the issues. There have been the reports on thermoresponsive MEMS switches based on bimorph configurations [6, 7]; however, these devices involved complex designs and/or relatively large sizes. Furthermore, they do not offer biocompatibility for their *in vivo* applications.

The shape-memory-alloy (SMA) based electrothermal actuators have been actively investigated

to show promising applications. The actuators that utilize nickel-titanium SMA known as nitinol, a proven biocompatible alloy, make them a favorable option for medical applications [8]. While SMA’s temporal response is relatively slow, SMA actuators provide large actuation forces, beneficial for lowering contact resistance and high-power handling, as well as high fatigue resistance to cyclic operation (well over a million of cycles) [9]; these features were exploited to develop high-power, low-frequency/DC micro contact switches [9]. Moreover, the use of SMA, a temperature-sensitive material, may enable a smart switch with a built-in sensing function that triggers in response to ambient temperature. Following this concept, a MEMS-based circuit breaker chip with an integrated thermoresponsive SMA switch [10] was developed to demonstrate the designed functionality. However, the relatively large chip size ($2.0 \times 1.5 \text{ mm}^2$) limited its application range. Downsizing the breaker chip is of paramount importance for not only minimizing its biological impact when implanted, but also enabling the chip integration with targeted smart implants whose available space is highly constrained as in many cases.

This study reports a circuit breaker microchip, enabled through further miniaturization of the preceding device based on the temperature-sensitive SMA switch, via improvements in the design and microfabrication while developing a packaging scheme that enhances the biocompatibility of the device. The targeted microchip is achieved to assist in greater integration density and size compatibility within the implanted surroundings, allowing its application to a wide range of *in vivo* microsystems that require thermoregulation for their safe operation (Figure 1). The particular focus of this development is placed on the application for smart active stents that are designed to electrothermally generate heat via wireless power transfer for endohyperthermia treatment of stented arteries [10], where the device space is extremely limited.

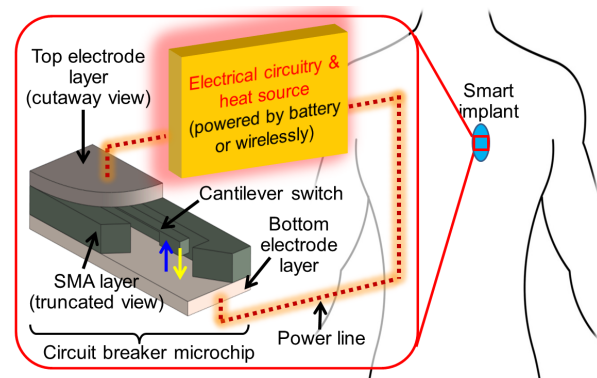


Figure 1: Conceptual view of the circuit breaker microchip coupled with an electrothermally active smart implant as an absolute temperature limiter that automatically regulates temperature of the implant.

DESIGN AND FABRICATION

The circuit breaker microchip investigated in this study is designed to have a bulk-micromachined nitinol cantilever beam that constitutes a temperature-sensitive contact switch, enclosed by a supporting frame of the same nitinol to define the chip's footprint of $0.7 \times 1.9 \text{ mm}^2$ (Figure 2). The cantilever structure ($1300 \times 100 \times 10 \text{ }\mu\text{m}^3$) within the frame is protected using planar bulk titanium layers that serve the dual functionality of packaging and electrical connection when bonded on both sides of the frame. A stressed silicon-dioxide reset layer prepared on top of the cantilever beam, which is flat at its memorized (austenitic) state, bends the beam down, while thin metal film wraps around the surfaces of the cantilever to ensure its good electrical contact with the substrate electrode. A cross sectional view of the microchip structure is shown in Figure 3(d). This microchip functions as a thermally triggered normally closed switch, which closes (ON) in its cold martensitic state but breaks the contact (OFF) upon reaching a temperature threshold due to the nitinol's phase transition to the austenitic state with which the cantilever moves back to the flat shape. By limiting the current flow that powers an implanted circuitry using this circuit breaker device, the heating process due to the current flow is interrupted to cool the circuitry down, at which the breaker automatically closes to power it again, enabling self-thermoregulation in electrothermally active implants. The bossed tip (with $80\text{-}\mu\text{m}$ thickness) is used in the cantilever design aiming to reduce the actuation distance and thus the cyclic switching time in the device.

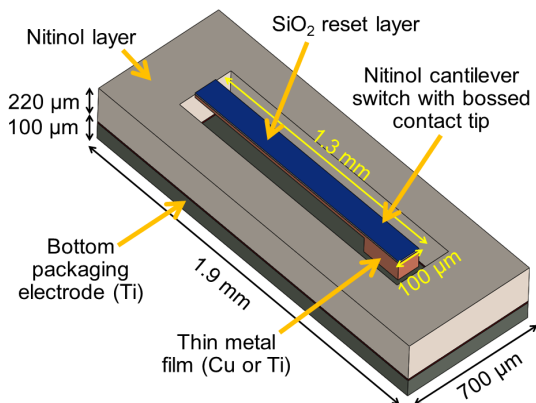


Figure 2: The design of the circuit breaker microchip with the top packaging electrode removed.

The designed breaker microchip is fabricated through a non-lithographic microfabrication process (Figure 3) developed to reduce process complexity while enabling ease of assembly for this miniaturized design. The process starts from micropatterning of a $220\text{-}\mu\text{m}$ -thick nitinol sheet (Alloy M, Memry, Germany; austenitic start temperature (A_s) = 56.5°C , austenitic peak temperature (A_p) = 68.5°C , martensitic start temperature (M_s) = 53.5°C) using micro-electro-discharge machining (μEDM , Figure 3(a)) to form the bossed-tip cantilever together with the frame structure that supports the cantilever. In this μEDM step, the surfaces of the nitinol cantilever are subjected to high-frequency thermal cycles due to instant heating induced by the localized discharge pulse and cooling by the dielectric machining fluid [11], causing a

residual (tensile) stress built into the processed surface layer thereby making the cantilever curl slightly. Prior to the subsequent step, this stressed surface layer is removed by etching the sample in hydrofluoric acid, which straightens the cantilever beam. Next, a silicon-dioxide layer with $4\text{-}5 \text{ }\mu\text{m}$ thickness is deposited on the top surface of the cantilever by plasma-enhanced chemical vapor deposition to serve as the reset layer (Figure 3(b)), which causes the beam to bend down due to a compressive stress of the layer; Figure 4(a) shows the bent cantilever (without the frame structure) after this step. The cantilever is then coated with a $\sim 200\text{-nm}$ -thick film of copper (with chromium adhesion layer) or titanium on both sides to reduce the series resistance of the beam as well as the contact resistance at its tip.

After these coatings, the nitinol layer is bonded to a piece of $100\text{-}\mu\text{m}$ -thick titanium foil (to be shaped later) that serves as the bottom packaging electrode; the inner surface of this layer is coated by either copper (as in the figure) or titanium with 200-nm thickness such that it creates the cantilever-electrode contact of the same material. This bonding step is performed using a ultraviolet (UV) sensitive liquid polyimide (HD-4100, HD Microsystems, USA) on the nitinol layer (temporarily fixed on a glass substrate; Figure 3(c)) through the following two steps: i) the nitinol actuator frame is coated with the liquid polyimide and cured to create an electrical insulation layer ensuring that no shorting between the nitinol frame and the electrode layer occurs when bonded together, and ii) the nitinol frame is coated with another layer of the same liquid polyimide that serves as the adhesive layer between the two components; the viscosity of this second layer is raised by exposing it to UV light for a short time to ease the bonding process. A sample after this bonding step is shown in Figure 4(b), displaying that the cantilever touches down on the bottom electrode. Another piece of titanium foil, which serves as the top packaging electrode (processed similarly as the bottom electrode), is then bonded on the other side of the nitinol frame using a combination of the liquid PI and a silver epoxy (CircuitWorks® Conductive Epoxy, Chemtronics, USA) to establish electrical connection between the nitinol and the top electrode. Finally, both top and bottom titanium layers are laser micromachined to achieve the microchip's final shape (Figure 3(d)).

Figure 4(c) shows a sample of the complete microchip. As noted earlier, the design of the microchip was aligned to its application to the smart stent, in which a tab-like structure with a size of $0.6 \times 2.0 \text{ mm}^2$ is arranged at one end of the stent structure as the platform for MEMS integration [12]. As illustrated in Figure 4(d), the packaged microchip fits well into this tab platform of the stent, and the reduction in chip footprint (by a factor of $\sim 2.3\times$ compared with the case reported in [10]) is evident. This size accommodation is a significant step towards achieving a clinically viable smart stent that not only maintains the biocompatibility required as a stent but also enables a low profile assembly when mounted on a delivery catheter (e.g., balloon catheter) for smooth insertion/navigation of the device into/through the arteries while preventing vascular injury during the procedure.

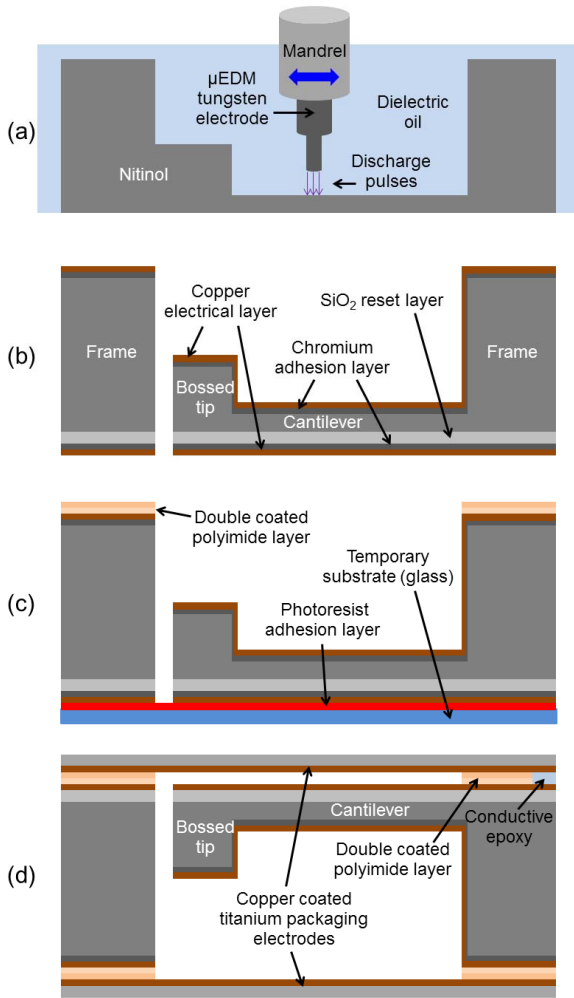


Figure 3: Microfabrication process: (a) μ EDM patterning of nitinol cantilever and chip frame; (b) PECVD of oxide reset layer and double-sided evaporation of copper (with chromium adhesion layer); (c) immobilization of nitinol layer and coating of polyimide insulation-bonding bilayer; (d) bonding and laser cutting of top and bottom titanium packaging electrode layers (inner surfaces pre-coated with copper) for final assembly.

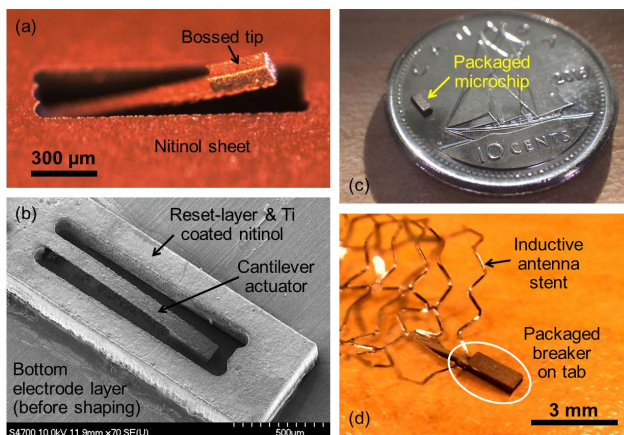


Figure 4: Microfabrication results: (a) nitinol cantilever with bossed tip; (b) microchip prior to the top electrode bonding; (c) fully packaged microchip (placed on a Canadian dime); (d) microchip mounted on the MEMS-integration platform of a smart stent device.

EXPERIMENTAL RESULTS

The thermomechanical and electrothermal responses of the fabricated breaker microchips were experimentally characterized using a controlled heat source. The set-up used for the former characterization is illustrated in Figure 5(a). The chip sample (without the top electrode to have an optical access to the cantilever) was secured on a hot plate whose temperature was monitored using a calibrated thermocouple. The deflections of the cantilever caused by elevated temperatures were tracked using a laser displacement sensor (LK-G32, Keyence Co., Japan) interfaced with its data acquisition unit connected to a computer. Figure 5(b) shows a typical response measured in a heating-cooling cycle. The result indicates that as temperature increased, the cantilever started to make a substantial upward motion at $\sim 54^\circ\text{C}$ in the heating path, reaching a full deflection of approximately $200\ \mu\text{m}$ at $\sim 67^\circ\text{C}$, and started to return downward at $\sim 56^\circ\text{C}$ in the cooling path. It should be noted that all the above temperature levels are consistent with A_s , A_p , and M_s of the particular nitinol material used, leading to a hysteresis response of the cantilever as displayed in the graph.

The electrical contact behavior of the breaker device is a critical characteristic as a microswitch. For the application targeted in this study, i.e., wirelessly powered electrothermal implants, an efficient power transfer and heating relies on a high electrical conductance of the breaker in its ON mode whereas the zero power transfer and cooling requires a fully open state in the OFF mode. The contact resistance behavior was characterized using a set-up similar to that shown in Figure 5(a), by electrically proving the device to track its resistance using a digital multimeter while varying device temperature.

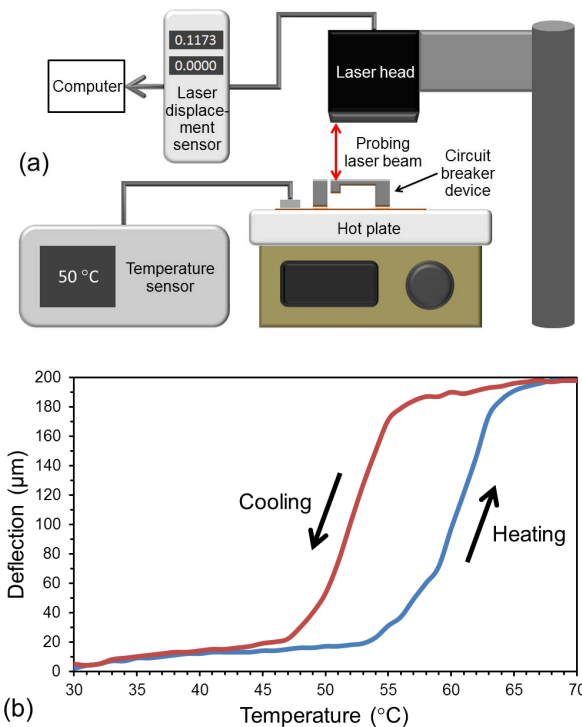


Figure 5: (a) The experimental set-up used for thermomechanical measurement of the fabricated breaker switch, and **(b)** displacements of the cantilever measured in a heating and cooling cycle.

Figure 6(a) displays a typical result measured using a fabricated breaker microchip with the copper-copper contact. The device exhibited a contact resistance of $\sim 35\ \Omega$ at the cold state, which started to rise rapidly when temperature exceeded $\sim 54\ ^\circ\text{C}$. This was followed by reaching a completely open condition at $\sim 65\ ^\circ\text{C}$, and upon cooling down towards room temperature, the contact resistance exhibited a rapid decrease at $\sim 55\ ^\circ\text{C}$ (these conditions are not shown in the graph) returning back to the nominal cold-state value. The threshold temperature levels observed along with the hysteretic electrical response matched well with those recorded in the thermochemical test discussed above. It was also found that the cold-state resistance and the dynamic contact behavior of the device with the titanium-titanium contact (Figure 6(b)) were almost identical to those of the copper-copper contact device. These experimental results verified the intended functionality of the developed circuit breaker microchip achieved in a highly miniaturized form.

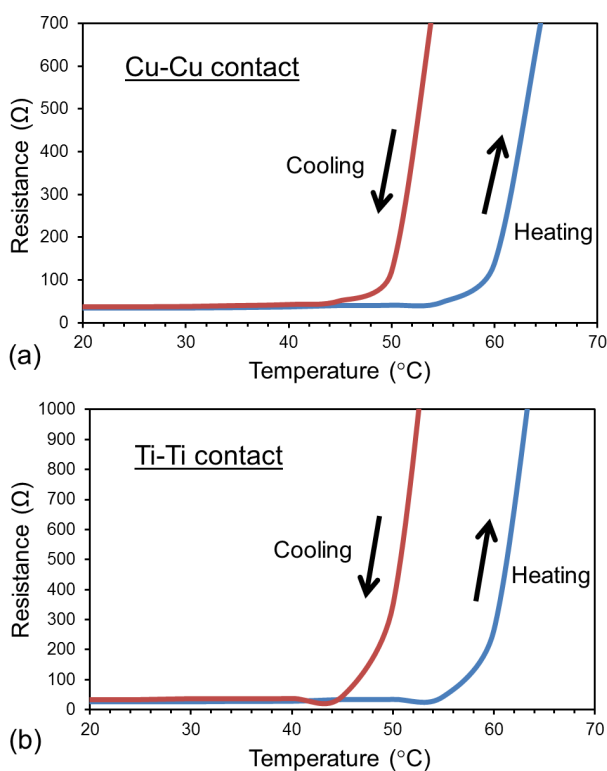


Figure 6: Electrothermal characteristics of the fabricated microchip with the electrical contact of (a) copper and (b) titanium, showing similar contact resistance behaviors and nominal levels at their cold states.

CONCLUSION

This study has investigated and developed a nitinol-based biocompatible circuit breaker microchip towards its application to smart implant devices requiring temperature management. The device was developed to achieve a substantial miniaturization compared with the preceding prototype though the new microswitch design and its microfabrication process. The electromechanical response of the fabricated microchips was experimentally characterized to reveal intended behaviors that matched well with the material properties of the nitinol material used, encouraging further development along the adopted

device design. Future work encompasses the adjustment of activation temperature tailored to a targeted application via using different types of nitinol with lower phase transition temperatures as well as the stability and reliability evaluation for design optimization.

ACKNOWLEDGMENTS

This work was partially supported by the Canadian Institutes of Health Research, the Natural Sciences and Engineering Research Council of Canada, the Canada Foundation for Innovation, and the British Columbia Knowledge Development Fund. K. Takahata is supported by the Canada Research Chairs program.

REFERENCES

- [1] K. Menon, R.A. Joy et al., "The applications of bioMEMS in diagnosis, cell biology, and therapy: a review," *BioNanoScience*, 4(4), pp. 356-366, 2013.
- [2] N.M. Elman, H.L. Ho Duc, M.J. Cima, "An implantable MEMS drug delivery device for rapid delivery in ambulatory emergency care," *Biomed. Microdev.*, 11(3), pp. 625-631, 2009.
- [3] X. Chen, D. Brox, B. Assadsangabi, Y. Hsiang, K. Takahata, "Intelligent telemetric stent for wireless monitoring of intravascular pressure and its *in vivo* testing," *Biomed. Microdev.*, 16(5), pp. 745-759, 2014.
- [4] P.S. Yarmolenko, E.J. Moon, C. Landon, A. Manzoor, D.W. Hochman, B.L. Viglianti, M.W. Dewhirst, "Thresholds for thermal damage to normal tissues: an update," *Int. J. Hyperther.*, 27(4), pp. 320-343, 2011.
- [5] Y. Luo, M. Dahmardeh, X. Chen, K. Takahata, "A resonant-heating stent for wireless endohyperthermia treatment of restenosis," *Sens. Actuators A*, 236, pp. 323-333, 2015.
- [6] X.Q. Sun, K.R. Farmer, W.N. Carr, "A bistable microrelay based on two-segment multimorph cantilever actuators," *IEEE MEMS*, pp. 154-159, 1998.
- [7] M.C. Gear, E.M. Yeatman et al., "Microengineered electrically resettable circuit breaker," *J. Microelectromech. Syst.*, 13(6), pp. 887-894, 2004.
- [8] C.D. Barras, K.A. Myers, "Nitinol - its use in vascular surgery and other applications," *Eur. J. Vasc. Endovasc. Surg. Syst.*, 19(6), pp. 564-569, 2000.
- [9] M. Dahmardeh, M.S. Mohamed Ali, T. Saleh et al., "High-power MEMS switch enabled by carbon-nanotube contact and shape-memory-alloy actuator," *Phys. Status Solidi A*, 210(4), pp. 631-638, 2013.
- [10] Y. Luo, M. Dahmardeh, K. Takahata, "Biocompatible circuit-breaker chip for thermal management of biomedical microsystems," *J. Micromech. Microeng.*, 25(5), 055002, 2015.
- [11] K. Takahata, "Micro-electro-discharge machining technologies for MEMS," in *Micro Electronic and Mechanical Systems*, In-Tech, 2009.
- [12] A.R. Mohammadi, M.S. Mohamed Ali, D. Lappin, C. Schlosser, K. Takahata, "Inductive antenna stent: design, fabrication, and characterization," *J. Micromech. Microeng.*, 23(2), 025015, 2013.

CONTACT

*A.L. Roy, email: roy13@ece.ubc.ca